Phosphorus Recovery From Waste Activated Sludge by Sponge Iron Seeded Crystallization of Vivianite and Process Optimization With Response Surface Methodology

Guoding Wu
Beijing University of Technology
Wei Zeng (zengwei@bjut.edu.cn)
Beijing University of Technology https://orcid.org/0000-0003-3429-4425
Shuaishuai Li
Beijing University of Technology
Ziyue Jia
Beijing University of Technology
Yongzhen Peng
Beijing University of Technology

Research Article

Keywords: Phosphorus recovery, Vivianite, Anaerobic fermentation, Seed crystal

Posted Date: March 15th, 2021

DOI: https://doi.org/10.21203/rs.3.rs-230136/v1

Abstract

As a novel phosphorus recovery product, vivianite ($Fe_3(PO_4)_2 \cdot 8H_2O$) has attracted much attention due to its enormous recycling potential and foreseeable economic value. Taking sponge iron as seed material, the effect of different reaction conditions on the recovery of phosphorus in waste activated sludge by vivianite crystallization was studied. Through single factor test, the optimal conditions for vivianite formation were in the pH range of 5.5–6.0 with Fe/P molar ratio of 1.5. Scanning electron microscopy (SEM), powder X-ray diffraction (XRD) and energy dispersive spectroscopy (EDS) were used to analyze the components of the crystals. The results showed that the vivianite produced with sponge iron as the seed crystal were larger and thicker (300-700 μm) than other seed (200-300 μm) and without seed (50-100 μm). Moreover, vivianite, which was synthesized with sponge iron as seed, was obviously magnetic and could be separated from sludge by rubidium magnet. The Box-Behnken design of the response surface methodology was used to optimize the phosphorus-recovery process with sponge iron (maximum phosphorus recovery rate was 83.17%), and the interaction effect of parameters was also examined. PH had a significant effect on the formation of vivianite. In summary, this research verifies the feasibility of using sponge iron as seed crystal to recover phosphorus in the form of vivianite from waste activated sludge, which is conducive to the subsequent separation and utilization of vivianite.

Introduction

Phosphorus (P) is a nutrient necessary for the circulation of substances in natural organisms and ecosystems. P is mainly stored in the earth's crust and is a non-renewable non-metallic mineral resource (Jalali and Jalali, 2016). Globally, the distribution of phosphate rock deposited on the earth is extremely uneven, and reserves are very limited. According to statistics, the phosphate mine may be exhausted after 50 years, and the risk of global food production is increased (Wu et al., 2019). The flow of phosphorus from the phosphate rock to the water environment is also a one-way process, which will undoubtedly lead to the loss of phosphorus and the eutrophication of the water (Falayi, 2019; Jia et al., 2020). Therefore, it is urgent to seek an efficient and reliable method of phosphorus recovery.

Waste activated sludge (WAS) is the largest phosphate storage except phosphate ore. Globally, 1.3 MT of phosphorus is stockpiled into the WAS every year through wastewater treatment plants(WWTPs)(Li and Li, 2017), which can meet 15–20% of the world's phosphorus demand if all the phosphorus is recycle (Zhiguo Yuan, 2012). Struvite as a widely studied phosphorus recovery product in the world, is limited by many influencing factors, such as magnesium source and pH. Complex process conditions also make the struvite recovery less than ideal (Cheng et al., 2017; Egle et al., 2015). Moreover, P recovery as struvite can only be conducted in the process of enhanced biological P removal (EBPR) of WWTPs (Wilfert et al., 2015). At the same time, iron as a commonly used chemical phosphorus removal agent was widely used in WWTPs, and the presence of vivianite ($Fe_3(PO_4)_2 \cdot 8H_2O$) in WAS is the main component of the ferrophosphorus compounds in the sludge. Vivianite as a fresh phosphorus recovery product began to receive widespread attention (Azam and Finneran, 2014; Hao Xiaodi, 2018; Wilfert et al., 2015).

Vivianite, often found in lake bottoms and ocean sediments, is a greatly stable ferrophosphorus compound with a high market value (approximate 10,000€/ton) (Wu et al., 2019). In addition to being the slow-release fertilizer,vivianite is a fundamental source for lithium iron phosphate ($LiFePO_4$) manufacturing, which is increasingly exploited as a precursor when fabricating Li-ion secondary batteries (Priambodo et al., 2017). At present, a large number of studies have confirmed the feasibility of applying vivianite precipitation into the sludge anaerobic system to recover phosphorus (Priambodo et al., 2017). Suitable concentrations of PO_4^{3-} and Fe^{2+} are required for the formation of vivianite. The results show that dissimilatory metal-reducing bacteria (DMRB), which is widely present in residual sludge, can convert Fe^{3+} added as phosphate removal agent into Fe^{2+} under reduction conditions (Wang et al., 2018). Moreover, wastewater contains a large amount of P when phosphate accumulating organisms (PAOs) and lysed microorganisms release P in an anaerobic environment (65–96 mg/L) and in the digester (137–177 mg/L). Compared with struvite (8.0-9.5), the formation of vivianite pH (6.0–9.0) is more suitable for recycling from WWTP, which does not require additional alkali leading to the increase of recycling cost (Liu et al., 2018). However, mixed vivianite particles (crystals and aggregates, size 10–150 mm) in the sludge is hard to separate, and many impurities change the vivianite characteristics (Wilfert et al., 2018). Therefore, it is necessary to find an effective strategy to increase the particle size of vivianite and improve its separation from WAS.

The formation of vivianite in the solution system is restricted by factors such as ambient temperature, solution supersaturation, ionic strength, and pH. These factors mainly affect the form and activity of ions, and thus affect the crystallization process of vivianite (Li et al., 2018). Introduction of seed induction or inhibition of primary nucleation at the early stage of precipitation crystallization is an effective means of crystallization (Peng et al., 2018). At present, most of the studies focus on recovering phosphorus from sludge superfluid to generate vivianite. However, the process is not only complicated, but also requires the addition of ferrous ions (Wu et al., 2019). In WWTP, most of the phosphorus and iron were deposited in WAS. Recovery of vivianite from sludge is a versatile phosphorus recovery method, and crystal seed can be added to improve the phosphorus recovery rate, which is rarely reported in this type of research.

This study adopted the sponge iron and iron hydroxide oxide (IHO) as additive seed of recycling vivianite, and the effects of different pH values, seed size and seed crystal dosage on the recovery of vivianite were explored. Additionally, the composition, morphology and settle ability of harvested vivianite crystals were analyzed by X-ray diffraction (XRD), scanning electron microscope (SEM) and zeta potential. To find interaction influence of elements on phosphorus recovery as vivianite, a response surface methodology (RSM) was used. The objectives of this study were to (i) investigate the existence form of phosphorus in sludge under different pH; (ii) prove the feasibility of phosphorus recovery by vivianite precipitation in the presence of seed crystal; and (iii) optimize the process conditions for the synthesis of vivianite with sponge iron as seed in sludge.

Materials And Methods

Waste activated sludge and chemicals

Sewage sludge was collected from the recycling sludge of secondary sedimentation tank in a lab-scale Modified University of Cape Town (MUCT) process, which is biological phosphorus removal without adding any chemical phosphorus removal agent. The withdrawn WAS was settled at room temperature for 12 h, and then, the supernatant was removed and the settled sludge was stored at 4°C. The mixed liquid suspended solids (MLSS) and mixed liquid volatile suspended solids (MLVSS) of the thickened WAS were 13.37 g/L and 8.52 g/L, respectively, while the soluble chemical oxygen demand (SCOD) were 79.23mg/L. The initial pH of WAS was 7.03 ± 0.1. The concentration of total Fe (TFe) and PO3- 4 were 8.09 mg/L and 318.64 mg/L. All chemicals used in this experiment were analysical reagent.

Seed crystal

Properties and chemical composition of sponge iron are shown in Table 1. Sponge iron also known as direct reducing iron, appearance gray black porous and mainly composed of elemental iron and iron oxide, can remove the dissolved oxygen in water (LI et al., 2009). Sponge iron was washed 3-5 times with distilled water to remove surface adhered particles and to be sure that there was no soluble salts. The washed sponge iron was then dried to a constant weight in an oven at 105 ℃ for 48 h, which was later converted into fine powder by a ball grinding mill. They were sieved with a 20-mesh (0.85 mm) particle size sieve. Finally, the fine powder was stored in a desiccator for further use.

All IHO used in this experiment were synthesized in the laboratory. First, a certain amount of $FeCl_3$ was dissolved in water and prepared into ferric chloride colloidal solution. 1 mol/L of NaOH was used to adjust the pH value of ferric chloride colloidal solution to 7. At this point, the dark red flocculent formed in the solution was ferric hydroxide. The supernatant was discharged after standing precipitation and washed with pure water. The operation was repeated until no Na^+ was detected, and then freeze-dry for 24 h and for use.

Batch experiments

The anaerobic digestion batch experiments were conducted with a reaction period of 20 days after adding substrate sludge and inoculated sludge in one time. Reaction container was 500 mL bottle of serum with a working volume a 400 mL. The volume ratio of substrate sludge and inoculated sludge was 1:3. Then pH value of mixed sludge was adjusted using 1 mol/L HCl and NaOH. After adding seed crystals and exogenous iron, the reactor (serum bottle) was aerated with pure nitrogen (N_2) for 5 min to discharge the dissolved oxygen and maintain the reactor anaerobic. Finally, the reactor was incubated in a constant temperature shaker (temperature 35°C, oscillating speed 160 r/min) away from light (Fig.1). The main parameters of batch tests were set as pH of 3.0, 4.0, 5.0 and 6.0, seed size of 100, 300 and 500 μm, and seed dosage of 3, 4 and 5 g/L. After the WAS fermentation the sludge was centrifuged and freeze-dried for 48 h. Rubidium magnets were then used to separate the seed coated with vivianite from the sludge.

Chemical analysis

The pH was determined by a pH meter (WTW Multi 340i□Germany). The sludge mixtures were sampled from the reactor and centrifuged at 5000 r/min for 5 min to separate the solids and supernatant. The centrifuged supernatant was filtered by 0.45 μm acetate fiber membrane for analysis. The concentration of MLSS, MLVSS, volatile fatty acid (VFA), Fe^{2+} and PO3- 4 were determined according to the standard methods (APHA, 2005). .For aqueous Fe^{2+} analysis, the centrifuged supernatant was immediately acidified using 1 mol/L HCl and determined within 1 h to prevent the oxidation.

In order to determine the variation of phosphorus fraction in sludge, the Standards, Measurements and Testing (SMT) protocol (Gonz Lez Medeiros et al., 2005) was adopted to identify the total phosphorus (TP), soluble phosphorus (SP), organic phosphorus (OP), non-apatite inorganic phosphorus (NAIP) and apatite phosphorus (AP). AP includes various inorganic phosphorus bound with Ca, while NAIP was combined with Fe, Mn, Al oxides and their hydroxides.

Characterization of the recovered precipitates

The scanning electron microscopy (SEM) coupled with energy dispersive spectrometer (EDS) (Hitachi S-4800, Japan) was used to analyze the micromorphology and elemental composition of recovered precipitates, while X-ray diffraction (XRD) (Bruker D8, Germany) was employed to determine the crystallographic structure of recovered precipitates with a scan rate of 6°/min in the scanning range (2θ) of 10-90° (Li et al., 2019). Co targets were used for XRD detection due to the magnetic properties of the samples.

Experimental Design for Response Surface Analysis

Response surface methodology (RSM) is a statistical method that seeks the optimal technological parameters through the analysis of response surface contours, and uses multiple quadratic regression to fit the functional relationship between factors and response values (Addagada, 2020). The response surface test was designed with Design-Expert 11 software as an auxiliary means and Box-Behnken Design model (BBD). The phosphorus recovery rate was used as response value (index value), and sponge iron was used as the seed crystal. Table 2 gives the code levels of each factor.

Results And Discussion

Effect of pH on P speciation without seed crystal

At the end of anaerobic fermentation, mixture samples were taken to analyze the P speciation. The variations of P speciation at different pH values without adding seed crystal were shown in Fig. 2a, pH is the key factors for efficient P recovery as vivianite, and different phosphorus distribution are formed at different pH values (Zhang et al., 2019). As shown in Fig.2a, when the pH was controlled at 6, phosphorus was mainly present in the solid phase, including NAIP (42.7%), AP (39.5%), and organic-P (11.6%).Notably, the NAIP proportion of 42.7% was the highest at pH 6.0, suggesting that this pH value was optimal for vivianite formation. With a decreasing pH, the solid-phase P species greatly decreased.

When the pH decreased to 3, the soluble orthophosphate became the main P species, increasing from 7.7% to 81.2%. On the contrary, the phosphorus removal efficiencies increased (82% to 98%) with the increase of pH. In the anaerobic fermentation process, except for the initial pH of 3, the pH value of other experimental groups showed a trend of first decreasing and then rising (Fig.2b). On the 4 d, the pH values of the groups with initial pH of 5 and 6 tended to be close and maintained the same growth trend until the end of anaerobic fermentation. Although the change trend of pH value of the two groups was similar, the content of vivianite in the two groups was significantly different after fermentation, which may be related to the lower ORP in the reaction process of the group with initial pH of 6. When the initial pH of 3, the whole environment showed strong acidity, which was beneficial to Eq.(2) but suppressed formula Eq.(3) (Wu et al., 2019). In addition, bioactivities of microorganisms involving in the formation of vivianite (DMRB, AOB, etc.) were also affected under the stimulation of over acidic environment, because these bacteria usually exist in neutral and weak acid environment (Schoepfer et al., 2019).

$$Fe(OH)_3 + 3H^+ + e^- \rightarrow 3H_2O + Fe^{2+} \quad (1)$$

$$3Fe^{2+} + 2PO_4^{3-} + 8H_2O \rightarrow Fe_3(PO_4)_2 \cdot 8H_2O \quad (2)$$

$$3Fe^{2+} + 2HPO_4^{2-} + 8H_2O \rightarrow Fe_3(PO_4)_2 \cdot 8H_2O + 2H^+ \quad (3)$$

Phosphate recovery as vivianite with sponge iron and IHO added

Previous studies indicated that weak acid conditions and low ORP were conducive to the formation of vivianite in WAS anaerobic fermentation (Liu et al., 2018). Nevertheless, the content of vivianite after the reaction was unsatisfactory, and its particle size (30-50 μm) was too small to be separated from the sludge. The addition of sponge iron and IHO suppresses the spontaneous formation of the initial crystal nucleus, and effectively increases the particle size of vivianite. Secondly, magnetic properties of sponge iron and IHO facilitate the subsequent recovery of vivianite. Thirdly, they can provide iron source Fe(Ⅱ) for DMRB. In this study, the concentrations of sponge iron and IHO were both 3 g/L with the Fe/P ratio of 1.5:1 and the initial pH of 6.

Variations of phosphate and divalent iron

To obtain high contaminants removal efficiency, adequate surface area and intension should be considered during the production process of sponge iron (LI et al., 2009). When electrochemistry reaction took place, Fe_2O_3 was transformed to Fe^{3+} or Fe^{2+}. Total dissolved phosphorus was further divided into inorganic (soluble reactive phosphorus) and organic (dissolved organic phosphorus) components. HPO2-4 and $H_2PO_4^-$ are commonly used to quantify total dissolved phosphorus (Wilfert et al., 2020). Fig.3 shows the variations of PO_3^{4+} and Fe^{2+} during anaerobic digestion of activated sludge with different seeds. In the initial stage of anaerobic fermentation, phosphate accumulating organisms (PAOs) took up VFAs and stored poly-hydroxybutrate (PHA), with energy derived mainly from the decomposition of intracellular polyphosphates (Poly-P). (Shi et al., 2019). As shown in Fig.3a, the phosphate concentration

rose in the initial stage due to the phosphorus release rate greater than the phosphorus settling rate, and then gradually decreased after reaching the peak on the fifth day. Phosphorus concentrations in the experimental group with IHO and sponge iron were 91.6 mg/L and 176.1 mg/L on the 20th day, which were significantly lower than the blank control group (385.7 mg/L). The results proved that when using $FeCl_3$ as a phosphorus removal agent, adding seed crystals effectively improved phosphorus adsorption. Compared with sponge iron, IHO had a smaller particle size and a larger specific surface area, and thus combined with more PO3- 4 in the sludge and made the phosphorus concentration lower.

In the WWTPs using polyferric chloride as chemical phosphorus removal reagent, there is a large amount of ferric chloride in the waste sludge. The increase of aqueous Fe^{2+} under acidic condition was primarily attributed to the biological Fe^{3+} reduction. Under anaerobic reduction conditions, Fe^{3+} is reduced to Fe^{2+} by DMRB (Vuillemin et al., 2013). The $FeCl_3$ in water was mainly hydrolyzed to form hydrous iron oxide (HFO) precipitates (Chen et al., 2019). As shown in Fig. 3b, with the initial pH of 6, the reaction system was weakly acidic, which was helpful to the reduction of Fe^{3+} and release of Fe^{2+}. The Fe^{2+} concentration with IHO reached the highest value of 73 mg/L on the 8th day, which reached the highest values of 73 mg/L and 66 mg/L on day 10 in the blank group and sponge iron group. The Fe^{2+} concentration in the blank group was higher than that of sponge iron. It was speculated that the porous structure and strong reducibility of sponge iron promoted the formation and adhesion of vivianite, so that Fe^{2+} and PO3- 4 in the system was consumed more.

Variations of VFA

The change of VFA concentration during the reaction is shown in Fig.3c. The VFA concentration of the raw sludge was 52.34 mg/L, and the VFA concentration rose rapidly at the initial stage of the reaction. The IHO group and sponge iron group reached their peaks (1016.8 mg/L, 1124.7 mg/L) on the 6th and 8th day, respectively, 19 times and 21 times the initial VFA concentration of sludge. Afterwards, the VFA concentration of IHO sludge dropped sharply and remained at a relatively stable level until the end of the reaction. The decrease of the VFA concentration in sponge iron sludge was relatively lagged, and the overall concentration was higher than that of IHO sludge. However, the VFA concentration of the experimental groups was much lower than that of control in the middle of the reaction, and only approached at the end of the experiment. Previous studies showed that the addition of zero-valent iron shortened the acidification stage of anaerobic fermentation and effectively inhibited the “over-acidification” in the sludge fermentation process (Kong et al., 2016). Zero-valent iron was used as an electron donor in the anaerobic digestion process. The organic acid generated in the acidificationstage caused hydrogen evolution corrosion, which stimulated the activity of methanogens and increased the methane production (Marin-Batista et al., 2020). Moreover, the galvanic cell composed of the iron-carbon component in the sponge iron theoretically accelerated the hydrogen evolution corrosion (Kong et al., 2018).

Characterization of phosphorus recovery products

XRD characterization analysis was performed on the crystals formed from IHO sludge and sponge iron sludge. The results are shown in Fig.4a. The two spectra represent the XRD diffraction results of the sludge in the digestion system with IHO and sponge iron in the temperature range of 10°~90°. Compared with the standard spectrum of vivianite (PDF#75-1186), a series of diffraction peaks of the crystals were basically consistent, indicating the crystal phase present in the sludge was vivianite. However, the presence of sponge iron and IHO changed the relative intensity of crystal diffraction peaks. The lattice plane relative strength of vivianite crystals (200 and -201) generated by spongy iron was slightly lower than that of IHO, implying that the morphology of vivianite could be changed by different seeds (Zhang et al., 2020).

This phenomenon was further confirmed by SEM images of vivianite crystal. In the absence of seed, the shape of harvested crystals was branched (Fig.4b), consistent with those reported in previous studies (Wang et al., 2018). Vivianite formed by spongy iron showed block-like and plate-like with dense structure (Fig.4c and Fig.4d). On the contrary, the vivianite generated in the reactor with IHO was irregular needle and bar structure (Fig. 4e, Fig.4f and Fig. 4g)，which was not found in previous studies (Zhang et al., 2020). The reason for the change in vivianite crystal morphology was possibly due to Fe^{2+} adsorbed onto the surface of sponge iron and IHO through static electricity, hydrogen bonding, chemical bonding and hydrophobicity (Rothe et al., 2016). Moreover, because sponge iron itself had strong magnetic properties, the vivianite produced with sponge iron as a seed crystal was also magnetic and could be easily adsorbed by neodymium magnet, and then be separated from the sludge (Prot et al., 2019). Fig.5 shows the crystal size of different seed crystals. The particle size of vivianite produced in the control group without seed crystals was 50-100 μm. The particle size of vivianite in IHO sludge and sponge iron sludge was 200-300 μm and 300-700μm, respectively. The vivianite generated by sponge iron was obviously larger. The change of vivianite crystal morphology will affect the utilization of P, which is worthy of further study.

RSM Scheme and Results

With seed dose of sponge iron (X_1), size of sponge iron (X_2), and pH value (X_3) as independent variables (Table 2), and phosphorus recovery efficiency as the response value (Y), the RSM experiment was performed. The experimental scheme and results are shown in Table 3, and the results of the model analysis of variance are shown in Table 4. After perform response surface analysis and quadratic regression fitting, the fitting equation was as following,

$$Y = 80.13 - 0.4225X_1 - 1.99X_2 + 7.06X_3 + 0.1225X_1X_2 - 0.7075X_1X_3 + 0.05X_2X_3 - 3.75X_1^2 - 2.27X_2^2 - 4.27X_3^2 \quad (4)$$

The Model F-value of 61.80 and P-value of <0.0001 implied the model was significant. There was only a 0.01% chance of such a large F-value due to noise. The coefficient R^2 value of 0.9876 suggested that only 1.24% of the dissimilarity existed between the experimental data and simulated data. The independent

variables X_2 (Size) and X_3 (pH) in the model had P values of 0.0010 and <0.0001, respectively, which had a significant influence on the phosphorus recovery efficiency, indicating that the model had a good fit.

Three-dimensional surface and contour plots of the phosphorus recovery are shown in Fig.6, which depicts the individual and interactive effects of the input factors (size, seed does, pH) on the phosphorus recovery. The strong impact of pH was possibly caused by two reasons. Firstly, the existing morphology and chemical equilibrium state of Fe and PO3- 4 could be changed by pH value, which affected the vivianite generation (Li et al., 2018). Secondly, DMRB, methanogenic bacteria, and methane anaerobic oxidizing bacteria involved in vivianite generation were prone to lose their bioactivities due to the influence of over-acid or over-alkali environment (Venkiteshwaran et al., 2018). The adsorption of phosphorus ions on sponge iron was mainly due to chemical binding, and thus the smaller the particle size (the larger the specific surface area), and the more favorable the adsorption of phosphorus and the formation of vivianite (Jiang et al., 2013). In this study, the particle size did not have a significant effect on the phosphorus recovery efficiency. That was due to that the sponge iron was ground by a ball mill, leading to the destruction of multi-pore honeycomb structure (Si et al., 2020). Moreover, the carbon component in sponge iron was separated, which affected the surface properties of the sponge iron and the electrochemical enrichment of primary cells on the surface of sponge iron. In addition, the seed dose of sponge iron had no significant effect on phosphorus recovery, which may be due to that the simultaneous addition of sponge iron and $FeCl_3$ made the iron in the system excessive. In subsequent studies, it is necessary to expand the gradient of the dosage to explore its effect on the formation of vivianite.

According to the response surface method, the optimal process parameters including the size of sponge iron of 213.56 μm, seed dose of 3.85 g/L and pH value of 5.84 were obtained after design optimization. In order to facilitate the experiment operation, the optimal parameters were adjusted as the size of 210 μm, the seed dose of 3.85 g/L, and the pH valueof 5.8. Under these conditions, the phosphorus recovery was repeated three times. The phosphorus recovery efficiency reached 82.13%, which was 1.4% different from the predicted value of 83.53%, and the relative error was 1.68%. The results showed that the model had high reliability and prediction accuracy, and could well simulated the formation conditions of vivianite.

Conclusion

In this study, phosphorous was recovered from WAS using vivianite precipitation with sponge iron dosing. The pH value had a significant effect on vivianite generation. As the pH increased, the content of vivianite in the sludge increased. The optimum pH for the generation of vivianite was found as 6. Addition of sponge iron improved the phosphorous recovery and obviously altered the morphology of vivianite. The addition of sponge iron not only effectively increased the particle size of vivianite, but also facilitated the subsequent separation and utilization of vivianite due to its own magnetism. Furthermore, the process optimization was performed using BBD of the response surface methodology. The optimal conditions predicted by the model are consistent with the response values under the experimental conditions, with a

dissimilarity of 1.4%. The maximum phosphorus recovery efficiency was 83.17%. In conclusion, the method of vivianite crystallization by adding sponge iron as seed crystal provides a novel and meritorious strategy for recovering phosphorus from WAS.

Declarations

Acknowledgements

This work was supported by the Natural Science Foundation of China [grant No.52070004] and Beijing Excellent Talents Project [grant No. 2017A36].

References

1. Addagada, L., 2020. Enhanced Phosphate Recovery Using Crystal-Seed-Enhanced Struvite Precipitation: Process Optimization with Response Surface Methodology. J. Hazard. Toxic Radioact. Waste 24, 4.
2. Azam, H.M., Finneran, K.T., 2014. Fe(III) reduction-mediated phosphate removal as vivianite (Fe3(PO4)2·8H2O) in septic system wastewater. Chemosphere 97, 1-9.
3. Chen, Y., Lin, H., Shen, N., Yan, W., Wang, J., Wang, G., 2019. Phosphorus release and recovery from Fe-enhanced primary sedimentation sludge via alkaline fermentation. Bioresource Technol 278, 266-271.
4. Cheng, X., Chen, B., Cui, Y., Sun, D., Wang, X., 2015. Iron(III) reduction-induced phosphate precipitation during anaerobic digestion of waste activated sludge. Sep Purif Technol 143, 6-11.
5. Cheng, X., Wang, J., Chen, B., Wang, Y., Liu, J., Liu, L., 2017. Effectiveness of phosphate removal during anaerobic digestion of waste activated sludge by dosing iron(III). J Environ Manage 193, 32-39.
6. Egle, L., Rechberger, H., Zessner, M., 2015. Overview and description of technologies for recovering phosphorus from municipal wastewater. Resources, Conservation and Recycling 105, 325-346.
7. Falayi, T., 2019. Alkaline recovery of phosphorous from sewage sludge and stabilisation of sewage sludge residue. Waste Manage 84, 166-172.
8. Gonz Lez Medeiros, J.J., P Rez Cid, B., Fern Ndez G Mez, E., 2005. Analytical phosphorus fractionation in sewage sludge and sediment samples. Anal Bioanal Chem 381, 873-878.
9. Hao Xiaodi, Z.J.W.C., 2018. New Product of Phosphorus Recovery——Vivianite. Acta Scientiae Circumstantiae 38(11), 4223-4234.
10. Jalali, M., Jalali, M., 2016. Relation between various soil phosphorus extraction methods and sorption parameters in calcareous soils with different texture. Sci Total Environ 566-567, 1080-1093.
11. Jia, Z., Zeng, W., Xu, H., Li, S., Peng, Y., 2020. Adsorption removal and reuse of phosphate from wastewater using a novel adsorbent of lanthanum-modified platanus biochar. Process Saf Environ 140, 221-232.

12. Jiang, C., Jia, L., He, Y., Zhang, B., Kirumba, G., Xie, J., 2013. Adsorptive removal of phosphorus from aqueous solution using sponge iron and zeolite. J Colloid Interf Sci 402, 246-252.
13. Kong, X., Wei, Y., Xu, S., Liu, J., Li, H., Liu, Y., Yu, S., 2016. Inhibiting excessive acidification using zero-valent iron in anaerobic digestion of food waste at high organic load rates. Bioresource Technol 211, 65-71.
14. Kong, X., Yu, S., Xu, S., Fang, W., Liu, J., Li, H., 2018. Effect of Fe0 addition on volatile fatty acids evolution on anaerobic digestion at high organic loading rates. Waste Manage 71, 719-727.
15. LI, J., LI, J., LI, Y., 2009. Cadmium removal from wastewater by sponge iron sphere prepared by charcoal direct reduction. Journal of environmental sciences (China) 21, S60-S64.
16. LI, J., LI, J., LI, Y., 2009. Cadmium removal from wastewater by sponge iron sphere prepared by charcoal direct reduction. Journal of environmental sciences (China) 21, S60-S64.
17. Li, L., Pang, H., He, J., Zhang, J., 2019. Characterization of phosphorus species distribution in waste activated sludge after anaerobic digestion and chemical precipitation with Fe3+ and Mg2+. Chem Eng J 373, 1279-1285.
18. Li, R., Cui, J., Li, X., Li, X., 2018. Phosphorus Removal and Recovery from Wastewater using Fe-Dosing Bioreactor and Cofermentation: Investigation by X-ray Absorption Near-Edge Structure Spectroscopy. Environ Sci Technol 52, 14119-14128.
19. Li, R., Li, X., 2017. Recovery of phosphorus and volatile fatty acids from wastewater and food waste with an iron-flocculation sequencing batch reactor and acidogenic co-fermentation. Bioresource Technol 245, 615-624.
20. Li, R., Wang, X., Li, X., 2018. A membrane bioreactor with iron dosing and acidogenic co-fermentation for enhanced phosphorus removal and recovery in wastewater treatment. Water Res 129, 402-412.
21. Liu, J., Cheng, X., Qi, X., Li, N., Tian, J., Qiu, B., Xu, K., Qu, D., 2018. Recovery of phosphate from aqueous solutions via vivianite crystallization: Thermodynamics and influence of pH. Chem Eng J 349, 37-46.
22. Marin-Batista, J.D., Mohedano, A.F., Rodríguez, J.J., de la Rubia, M.A., 2020. Energy and phosphorous recovery through hydrothermal carbonization of digested sewage sludge. Waste Manage 105, 566-574.
23. Peng, L., Dai, H., Wu, Y., Peng, Y., Lu, X., 2018. A comprehensive review of phosphorus recovery from wastewater by crystallization processes. Chemosphere 197, 768-781.
24. Priambodo, R., Tan, Y., Shih, Y., Huang, Y., 2017. Fluidized-bed crystallization of iron phosphate from solution containing phosphorus. J Taiwan Inst Chem E 80, 247-254.
25. Prot, T., Nguyen, V.H., Wilfert, P., Dugulan, A.I., Goubitz, K., De Ridder, D.J., Korving, L., Rem, P., Bouderbala, A., Witkamp, G.J., van Loosdrecht, M.C.M., 2019. Magnetic separation and characterization of vivianite from digested sewage sludge. Sep Purif Technol 224, 564-579.
26. Rothe, M., Kleeberg, A., Hupfer, M., 2016. The occurrence, identification and environmental relevance of vivianite in waterlogged soils and aquatic sediments. Earth-Sci Rev 158, 51-64.

27. Schoepfer, V.A., Burton, E.D., Johnston, S.G., Kraal, P., 2019. Phosphate loading alters schwertmannite transformation rates and pathways during microbial reduction. Sci Total Environ 657, 770-780.
28. Shi, Y., Luo, G., Rao, Y., Chen, H., Zhang, S., 2019. Hydrothermal conversion of dewatered sewage sludge: Focusing on the transformation mechanism and recovery of phosphorus. Chemosphere 228, 619-628.
29. Si, Z., Song, X., Wang, Y., Cao, X., Wang, Y., Zhao, Y., Ge, X., Sand, W., 2020. Untangling the nitrate removal pathways for a constructed wetland- sponge iron coupled system and the impacts of sponge iron on a wetland ecosystem. J Hazard Mater 393, 122407.
30. Venkiteshwaran, K., Pokhrel, N., Hussein, F., Antony, E., Mayer, B.K., 2018. Phosphate removal and recovery using immobilized phosphate binding proteins. Water Research X 1, 100003.
31. Vuillemin, A., Ariztegui, D., De Coninck, A.S., Lücke, A., Mayr, C., Schubert, C.J., 2013. Origin and significance of diagenetic concretions in sediments of Laguna Potrok Aike, southern Argentina. J Paleolimnol 50, 275-291.
32. Wang, S., An, J., Wan, Y., Du, Q., Wang, X., Cheng, X., Li, N., 2018. Phosphorus Competition in Bioinduced Vivianite Recovery from Wastewater. Environ Sci Technol 52, 13863-13870.
33. Wilfert, P., Dugulan, A.I., Goubitz, K., Korving, L., Witkamp, G.J., Van Loosdrecht, M.C.M., 2018. Vivianite as the main phosphate mineral in digested sewage sludge and its role for phosphate recovery. Water Res 144, 312-321.
34. Wilfert, P., Kumar, P.S., Korving, L., Witkamp, G., van Loosdrecht, M.C.M., 2015. The Relevance of Phosphorus and Iron Chemistry to the Recovery of Phosphorus from Wastewater: A Review. Environ Sci Technol 49, 9400-9414.
35. Wilfert, P., Meerdink, J., Degaga, B., Temmink, H., Korving, L., Witkamp, G.J., Goubitz, K., van Loosdrecht, M.C.M., 2020. Sulfide induced phosphate release from iron phosphates and its potential for phosphate recovery. Water Res 171, 115389.
36. Wu, Y., Luo, J., Zhang, Q., Aleem, M., Fang, F., Xue, Z., Cao, J., 2019. Potentials and challenges of phosphorus recovery as vivianite from wastewater: A review. Chemosphere 226, 246-258.
37. Zhang, B., Wang, L., Li, Y., 2019. Fractionation and identification of iron-phosphorus compounds in sewage sludge. Chemosphere 223, 250-256.
38. Zhang, C., Hu, D., Yang, R., Liu, Z., 2020. Effect of sodium alginate on phosphorus recovery by vivianite precipitation. J Environ Sci-China 93, 164-169.
39. Zhiguo Yuan, S.P.A.D., 2012. Phosphorus recovery from wastewater through microbial processes. Curr. Opin. Biotechnol 23 (6), 878-883.

Tables

Table 1 Properties and chemical composition of sponge iron

Items		Value
Properties	specific surface area (g/cm^3)	85
	Volumetric weight (g/cm^3)	2.2
Chemical composition	FeO	≥95%
	SiO_2	≤2.5%
	Al_2O_3	≤2.0%
	SOx	≤0.03%

Table 2 The design of orthogonal experiment

			Levels		
No.	Code	Factors	-1	0	1
1	X_1	Seed dose (g/L)	3	4	5
2	X_2	Size (μm)	100	300	500
3	X_3	pH	4	5	6

Table 3 Box–Behnken matrix and the corresponding response values

Run	Factor 1 X_1:Seed dose(g/L)	Factor 2 X_2:Size(μm)	Factor 3 X_3:pH	Phosphorus recovery efficiency(%)
1	4	300	5	80.31
2	3	300	4	64.92
3	5	300	6	77.88
4	5	300	4	65.3
5	4	100	4	69.02
6	3	100	5	76.02
7	4	500	6	78.25
8	4	100	6	82.17
9	3	300	6	80.33
10	4	300	5	78.82
11	4	500	4	63.9
12	3	500	5	72.84
13	5	500	5	72.43
14	4	300	5	81.91
15	4	300	5	79.44
16	4	300	5	80.15
17	5	100	5	75.12

Table 4 Analysis of variance for the quadratic model

Source	Sum of squares	df	Mean square	F-value	P-value
Model	608.75	9	67.64	61.72	<0.0001
X_1-Seed dose	1.43	1	1.43	1.30	0.2912
X_2-Size	31.64	1	31.64	28.87	0.0010
X_3-pH	398.89	1	398.89	363.97	<0.0001
X_1X_2	0.0600	1	0.0600	0.0548	0.8217
X_1X_3	2.00	1	2.00	1.83	0.2185
X_2X_3	0.0100	1	0.0100	0.0091	0.9266
X_1^2	59.23	1	59.23	54.04	0.0002
X_2^2	21.75	1	21.75	19.85	0.0030
X_3^2	76.70	1	76.70	69.98	< 0.0001
Residual	7.67	7	1.10	—	—
Lack of Fit	2.28	3	0.7594	0.5632	0.6675
Pure Error	5.39	4	1.35	—	—
Cor Total	616.42	16	—	—	—

Figures

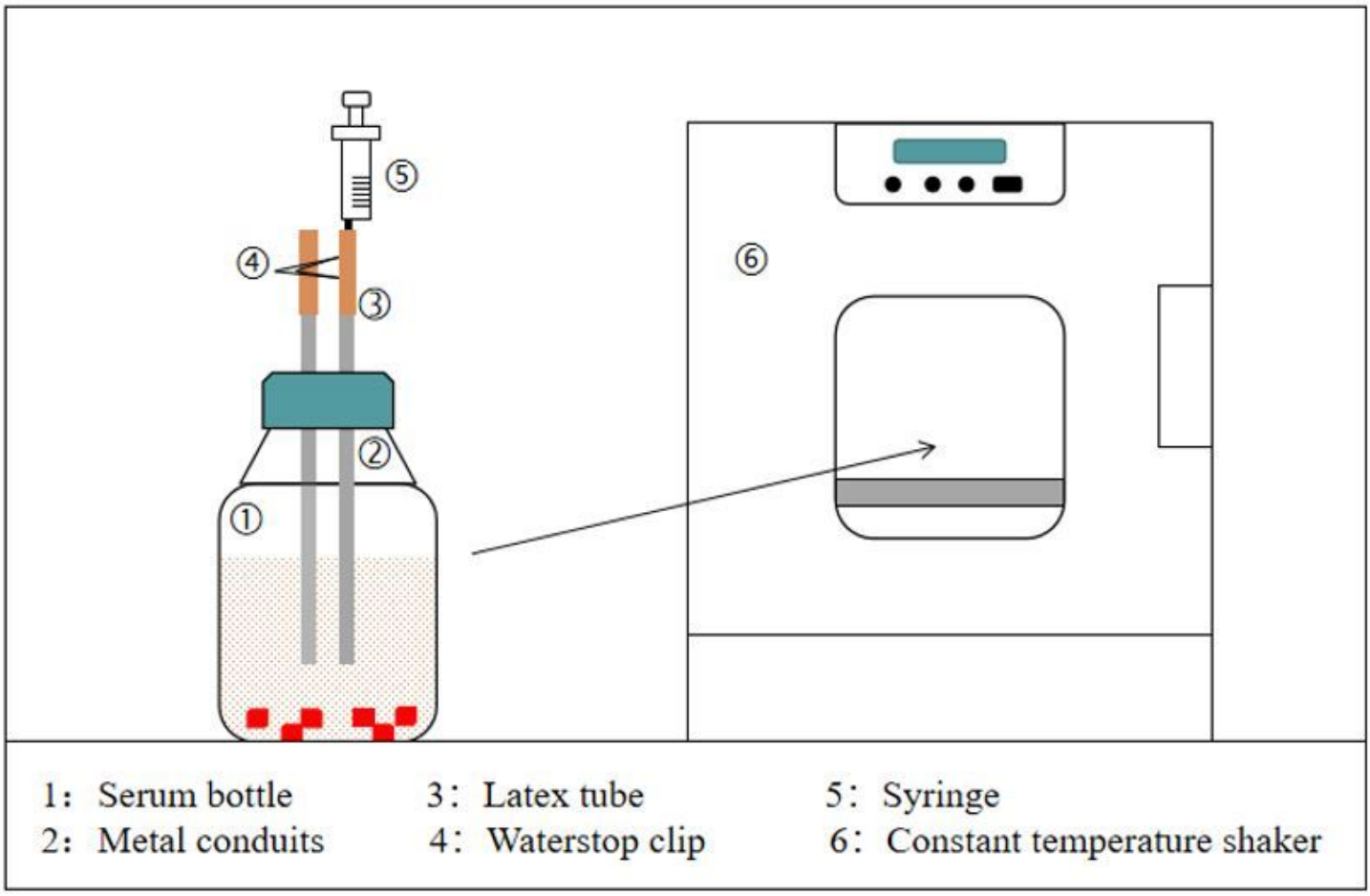

Figure 1

Schematic diagram of the experimental rig for vivianite crystallization.

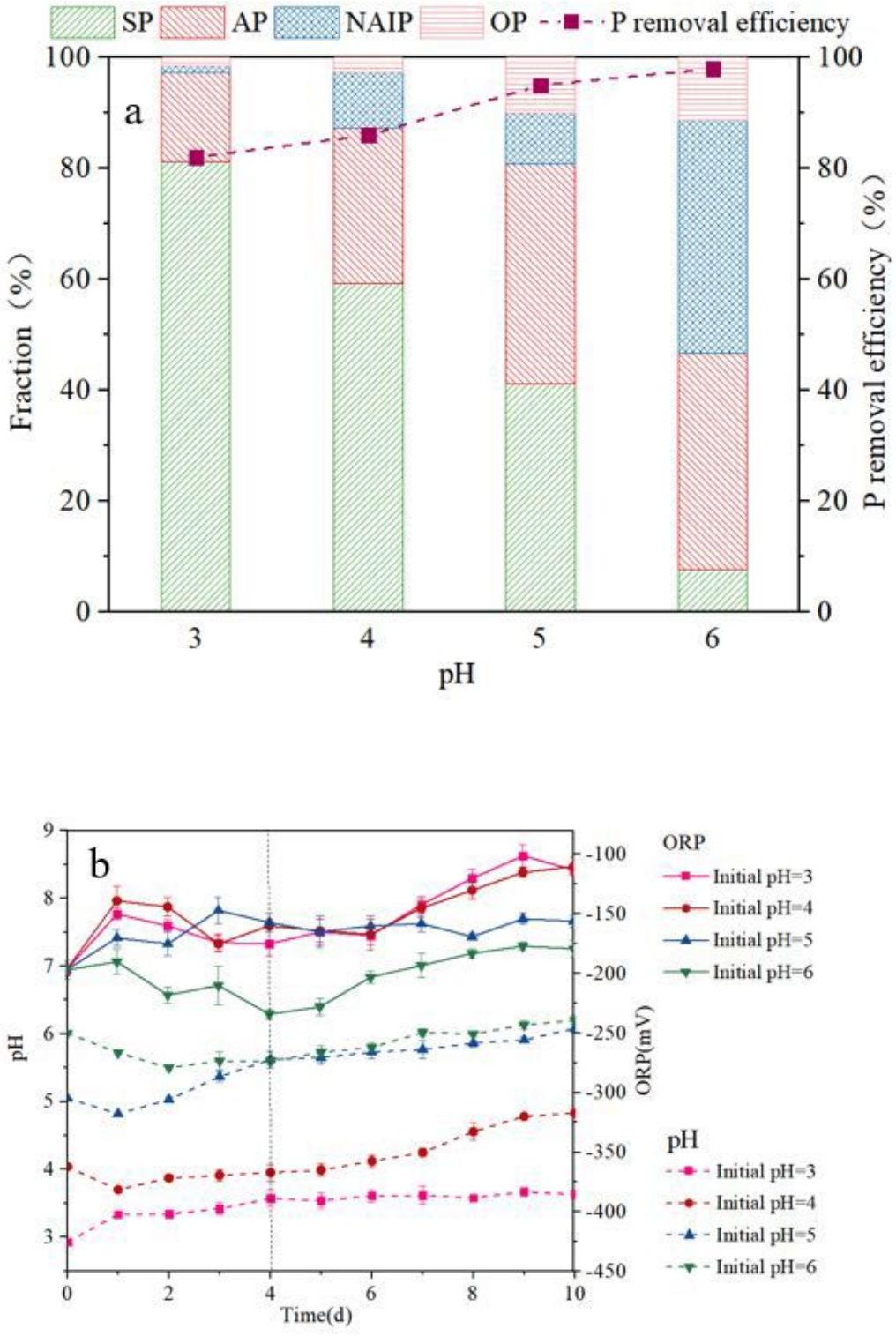

Figure 2

(a) P speciation characterized by the chemical measurements on the sludge samples as a function of the pH ; (b) Variation of pH and ORP during the anaerobic digestion of sludge.

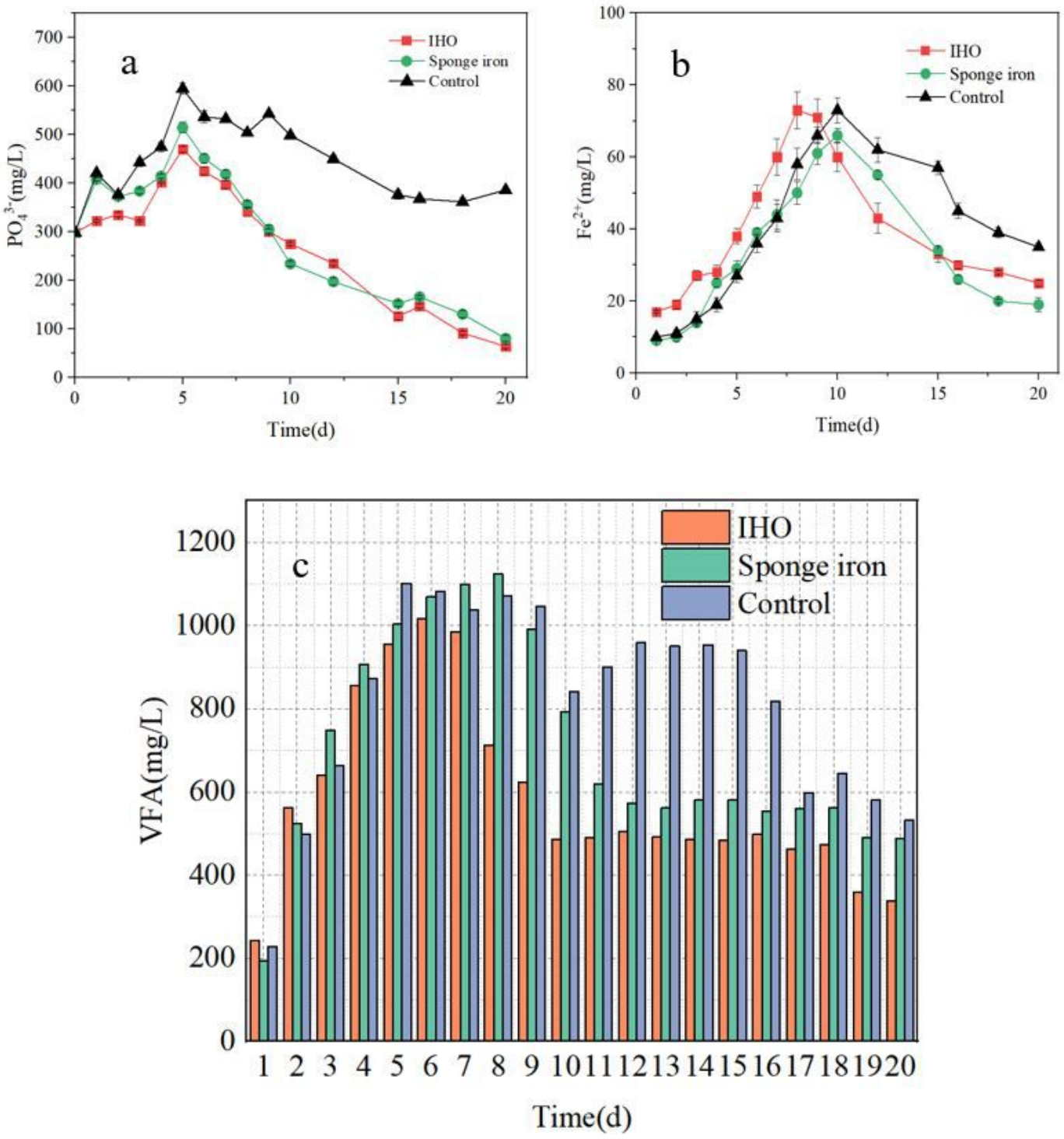

Figure 3

Variation of (a) PO43-, (b) Fe2+ and (c) VFA during anaerobic digestion of activated sludge with different seed crystal.

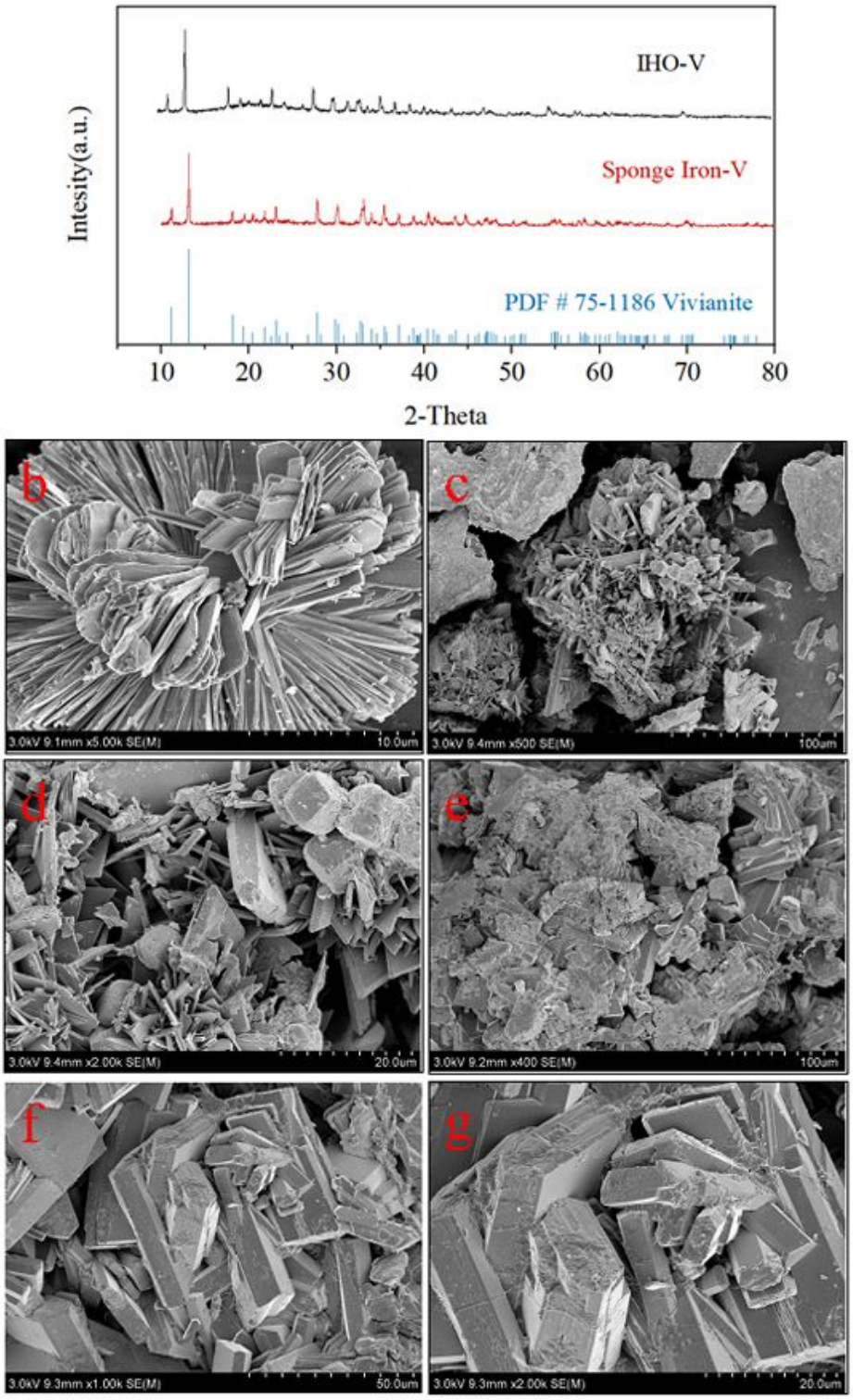

Figure 4

(a) XRD spectra and (b-g) SEM imagesof recovered products with different seeds.

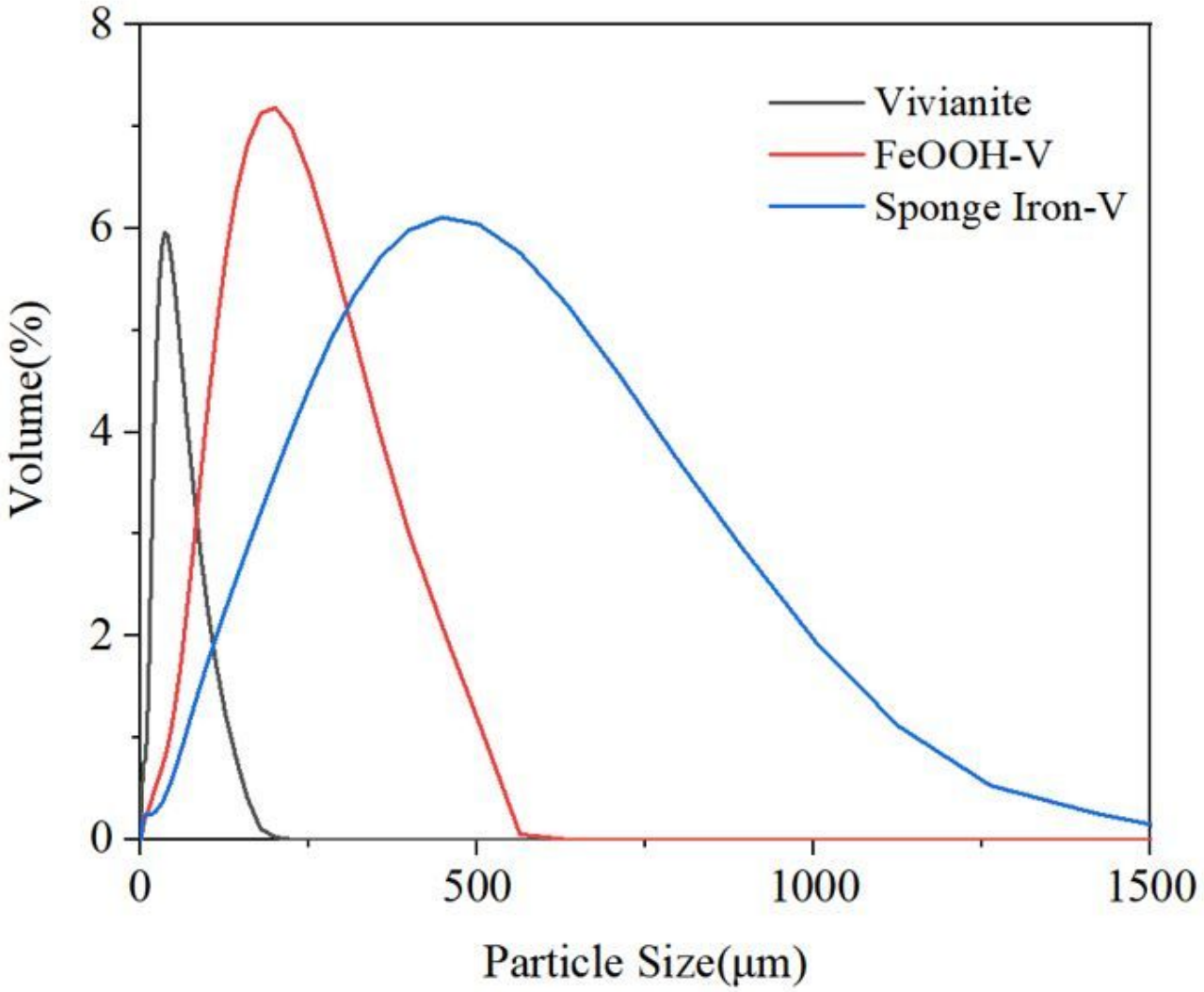

Figure 5

Particle sizes of recovered crystals with different seeds.

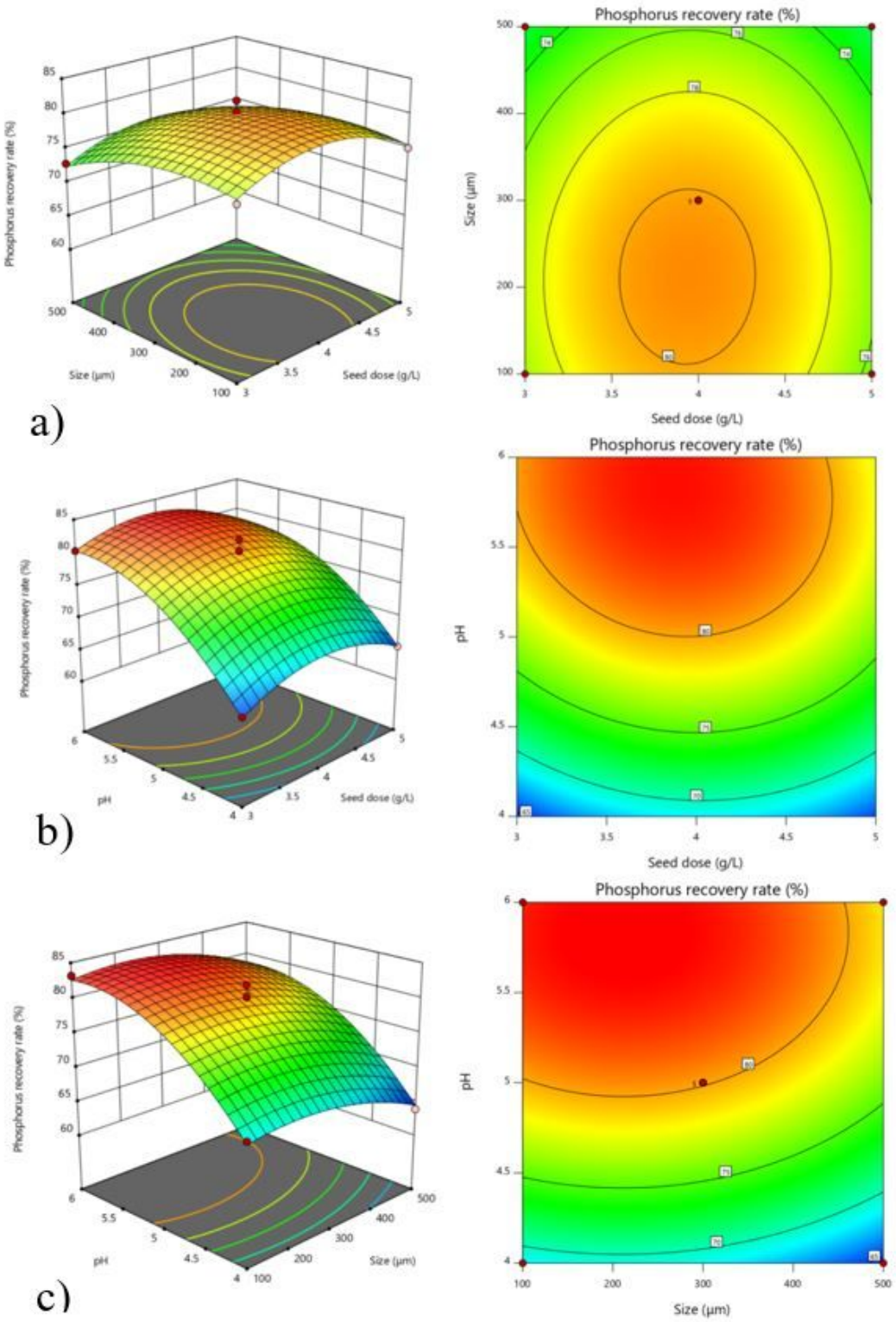

Figure 6

Interaction influence of a) size and seed dose; b) pH and seed dose; c) pH and size on phosphorus recovery rate.